

HISTORY AND PROGRESS OF THE TOW–THOMAS BI-QUADRATIC FILTER. PART I. GENERATION AND OP AMP REALIZATIONS

AHMED M. SOLIMAN

*Electronics and Communication Engineering Department,
Cairo University, Egypt 12613
asoliman@ieee.org*

Revised 10 April 2007

The history of Tow–Thomas second-order filter is reviewed. Two alternative generation methods of the Tow–Thomas filter are discussed. The first is a generation method from the second-order passive RLC filter and the second is from the multiple feedbacks inverting low-pass filter using a single op amp. Several forms of the circuit are briefly reviewed. Passive and active compensation methods to improve the circuit performance for high- Q designs are summarized. Spice simulation results are included.

Keywords: Active filters; operational amplifier circuits; Tow–Thomas filter.

1. Introduction

One of the most famous active filter circuits is the Tow–Thomas bi-quadratic circuit (TT-biquad).^{1,2} This circuit is included almost in all textbooks in active filters,^{3–10} and is introduced in most universities to the undergraduate or graduate students. Although the circuit was introduced since 38 years it is still receiving interest of researchers in modifying it to fit the new CMOS technology.^{11–13} Due to the great importance of this circuit and the progress in its realization it is desirable to collect such progress in a review paper, this is the objective of this paper. It is hoped that this paper will be of value to professors teaching this circuit and to designers of active filters.

2. The Origin of the Tow–Thomas Filter Circuit

Although the circuit is well known by the names of the two persons it is important to know the original history of the circuit. The circuit was first introduced by Tow.¹ In his paper, he introduced five circuits to realize different filter responses low-pass, band-pass using three op amps and then high-pass, all-pass and notch using four op amps. Thomas independently submitted his paper² in 1 July 1969 before Tow circuit was published in December 1969; that is why the circuit is known by both names.

Thomas² started his paper with the biquad circuit in its general form using four op amps. The paper discussed the Q enhancement caused by finite gain bandwidth of the op amp and it was among the first papers¹⁴ discussed this very important topic. The TT circuit can be generated from passive RLC filter or from the multiple feedbacks inverting low-pass filter as will be shown next.

2.1. Generation of TT circuit from passive RLC circuit

Figure 1(a) represents the passive RLC filter, realizing a low-pass output response at the capacitor C terminal. The transfer function is given by

$$\frac{V_{LP}}{V_I} = \frac{1}{s^2 LC + sCR + 1}. \quad (1)$$

This transfer function can be represented by the block diagram shown in Fig. 1(b).¹⁵ The block diagram can be represented by two cascaded lossy integrator and lossless integrator as shown in Fig. 1(c), where for the passive RLC circuit in Fig. 1(a), the time constants τ_1 and τ_2 are given by

$$\tau_1 = \frac{L}{R}, \quad \tau_2 = CR. \quad (2)$$

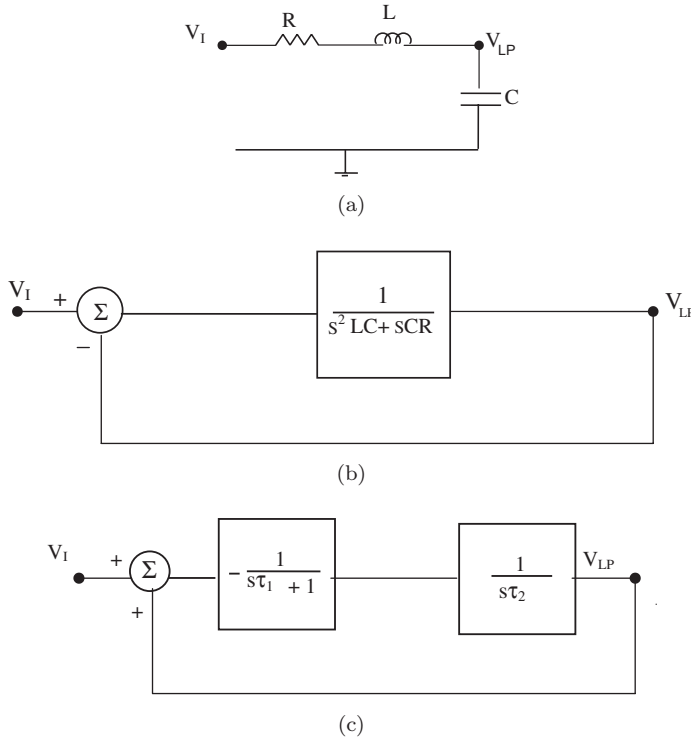


Fig. 1. (a) The passive RLC low-pass filter. (b) A block diagram of (a). (c) An equivalent block diagram to that of (b).

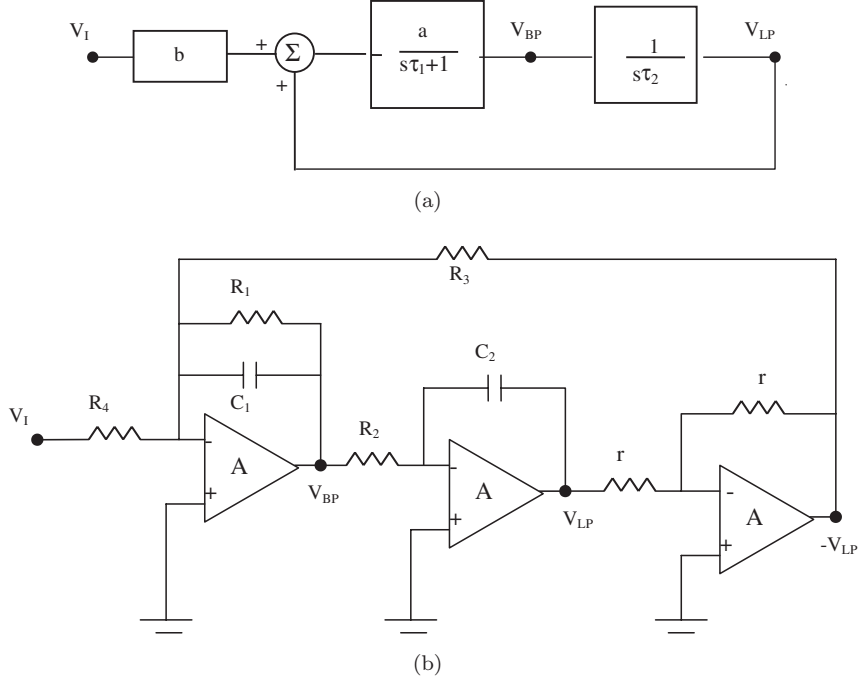


Fig. 2. (a) A modified block diagram to that of Fig. 1(c). (b) The Tow–Thomas circuit.^{1,2}

Next, some modifications are introduced to this block diagram by adding the parameters a, b to provide degrees of freedom in controlling the gain and the Q factor of the active filter. The modified block diagram is shown in Fig. 2(a) and its transfer functions are given by

$$\frac{V_{BP}}{V_I} = \frac{\frac{-ab}{\tau_1} s}{s^2 + \frac{1}{\tau_1} s + \frac{a}{\tau_1 \tau_2}}, \quad (3a)$$

$$\frac{V_{LP}}{V_I} = \frac{\frac{-ab}{\tau_1 \tau_2}}{s^2 + \frac{1}{\tau_1} s + \frac{a}{\tau_1 \tau_2}}. \quad (3b)$$

The block diagram in Fig. 2(a) is practically realizable to give the well-known TT biquad shown in Fig. 2(b), drawn here with the R and C suffixes as in Thomas paper exactly.² From Figs. 2(a) and 2(b) it can be seen that:

$$\tau_1 = C_1 R_1, \quad \tau_2 = C_2 R_2, \quad a = \frac{R_1}{R_3}, \quad b = \frac{R_3}{R_4}. \quad (4)$$

The band-pass and the low-pass transfer functions are given, respectively, by

$$\frac{V_{BP}}{V_I} = \frac{\frac{-s}{C_1 R_4}}{s^2 + \frac{s}{C_1 R_1} + \frac{1}{C_1 C_2 R_2 R_3}}, \quad (5a)$$

$$\frac{V_{LP}}{V_I} = \frac{\frac{1}{C_1 C_2 R_2 R_4}}{s^2 + \frac{s}{C_1 R_1} + \frac{1}{C_1 C_2 R_2 R_3}}. \quad (5b)$$

From the above equations it is seen that the ω_0 and Q are given by

$$\omega_0 = \frac{1}{\sqrt{C_1 C_2 R_2 R_3}}, \quad Q = R_1 \sqrt{\frac{C_1}{C_2 R_2 R_3}}. \quad (6)$$

The magnitude of the gain at ω_0 at the band-pass output is given by $T(\omega_0) = R_1/R_4$. The magnitude of DC gain at both of the low-pass outputs is given by $T(0) = R_3/R_4$.

Taking $C_1 = C_2 = C$, $R_2 = R_3 = R$, the design equations for a specified ω_0 and Q are given by

$$R_1 = QR, \quad R = \frac{1}{\omega_0 C}. \quad (7)$$

For a specified band-pass center frequency gain $T(\omega_0)$, the design equation for R_4 is given by

$$R_4 = \frac{R_1}{T(\omega_0)}. \quad (8)$$

For a specified DC gain $T(0)$, the design equation for R_4 is given by

$$R_4 = \frac{R}{T(0)}. \quad (9)$$

2.2. Generation of TT circuit from a single op amp low-pass filter

Figure 3(a) represents the single op amp multiple feedback inverting low-pass filter.³ Applying Kirchhoff current law (KCL) at the band-pass node results in:

$$V_I G_4 + V_{LP} G_3 = V_{BP} (G_2 + G_3 + G_4 + sC_1). \quad (10)$$

Let

$$G_1 = G_2 + G_3 + G_4. \quad (11)$$

Equation (10) can be realized by the first two stages of Fig. 3(b) (in which V_{BP} is negative) which when combined with the second inverting integrator results in a version of the TT circuit shown in Fig. 3(b). The resistor R_1 can now be taken arbitrary and different from the value given by Eq. (11). The design equations are the same as given by Eq. (7). The circuit in Fig. 3(b) has two band-pass outputs one inverting and one noninverting and has only one inverting low-pass output. That is the main difference from the TT circuit shown in Fig. 2(b).

2.3. Modified forms of Tow–Thomas circuit

An alternative form of TT circuit was also introduced in Ref. 16 by adding the resistor R_5 as shown in the circuit in Fig. 3(c). The circuit has one inverting

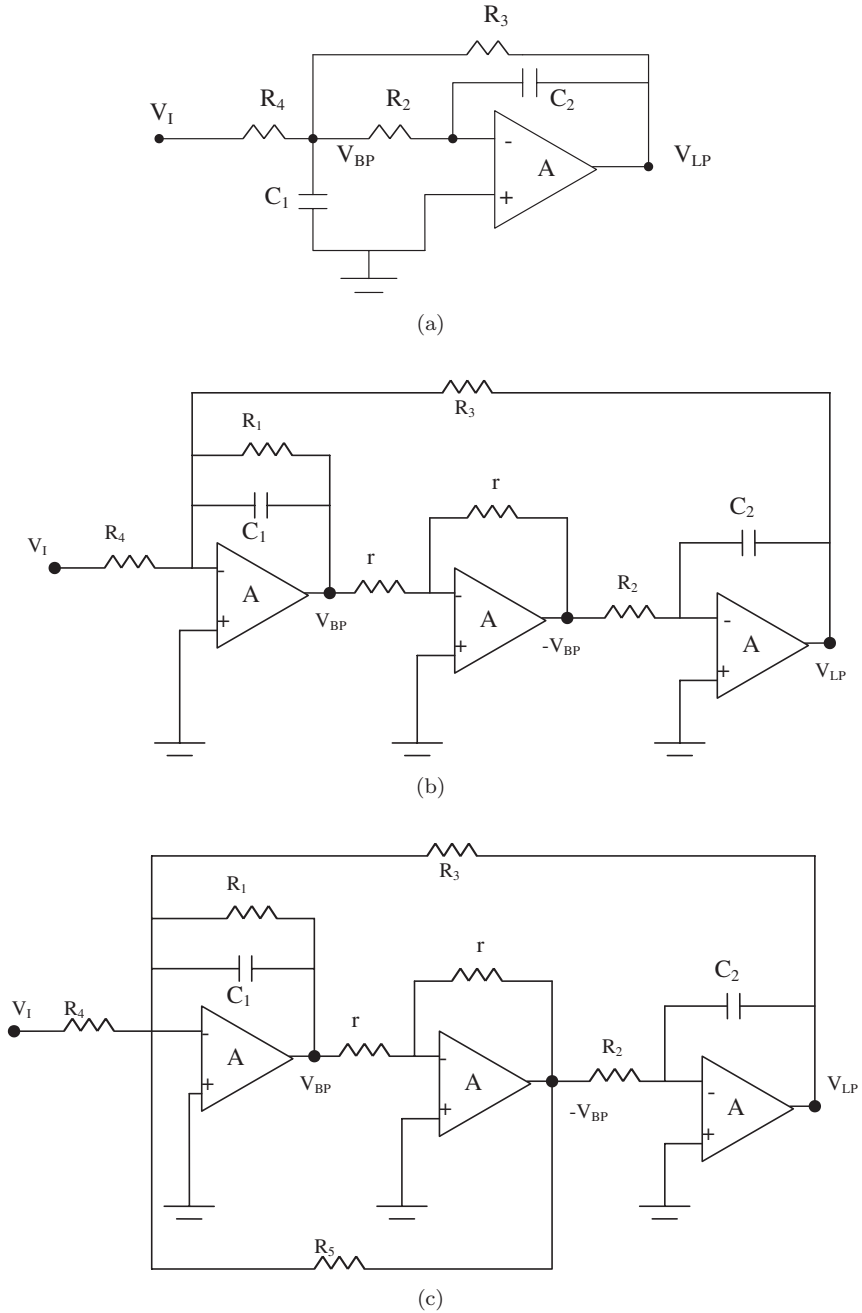


Fig. 3. (a) The single op amp multiple feedback low-pass filter.³ (b) Alternative form of Tow–Thomas circuit.¹⁶ (c) A modified form of the circuit in (b).¹⁶ (d) Modified Tow–Thomas circuit using Deboo integrator.^{2,14}

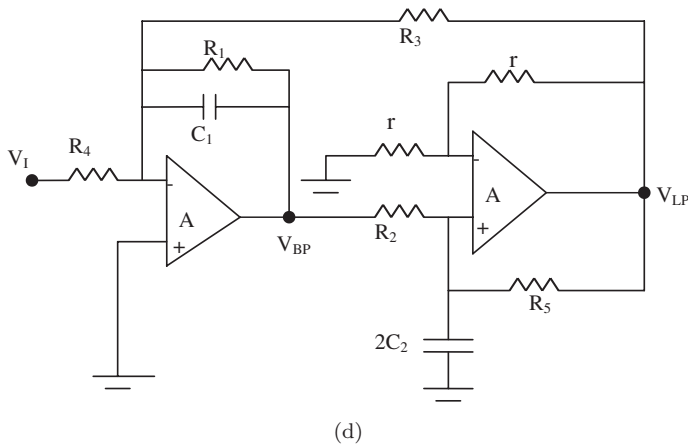


Fig. 3. (Continued)

low-pass output and two opposite polarity band-pass outputs. The circuit equations are given by

$$\frac{V_{BP}}{V_I} = \frac{\frac{-s}{C_1 R_4}}{s^2 + \frac{s}{C_1} \left(\frac{1}{R_1} - \frac{1}{R_5} \right) + \frac{1}{C_1 C_2 R_2 R_3}}, \quad (12a)$$

$$\frac{V_{LP}}{V_I} = \frac{\frac{-1}{C_1 C_2 R_2 R_4}}{s^2 + \frac{s}{C_1} \left(\frac{1}{R_1} - \frac{1}{R_5} \right) + \frac{1}{C_1 C_2 R_2 R_3}}. \quad (12b)$$

It is seen that the resistors R_1 and R_5 control Q of the filter which can be made high when the two resistors approach each other in value. The subtraction, however, in the s term results in a high- Q sensitivity to R_1 and R_5 and is given by

$$\frac{Q}{S_{R_1}} = -\frac{Q}{S_{R_5}} = \frac{Q}{\omega_0 C_1 R_1}. \quad (13)$$

It should be noted that the original TT circuit shown in Fig. 2(b) has all the ω_0 and Q passive sensitivities to all passive circuit components being less than or equal to 1.

A modified form of the Tow–Thomas circuit based on Deboo grounded capacitor noninverting integrator is shown in Fig. 3(d).^{2,14} The circuit uses one op amp less than the original Tow–Thomas circuit and realizes inverting band-pass and inverting low-pass responses as shown in Table 1. A necessary condition for the noninverting integrator is that $R_5 = R_2$. The circuit has high passive Q sensitivity to R_5 and R_2 and for independent control on Q these two resistors must be equal. In Ref. 14 the circuit was used without the feedback resistor R_1 and in this case there is no independent control on Q .

Table 1. Comparison of the Tow–Thomas biquad and the modified circuits.

Circuit figure	Op amps	C	R	Independent control on Q	Band-pass polarity	Low-pass polarity
2b	3	2	6	Yes by R_1	Inverting	Both polarities
3b	3	2	6	Yes by R_1	Both polarities	Inverting
3c	3	2	7	Yes by R_1 or R_5	Both polarities	Inverting
3d	2	2	7	Yes by R_1	Inverting	Inverting
4a	4	2	9	No	—	Both polarities
4b	3	2	7	No	—	Both polarities
4c	3	2	7	No	—	Both polarities
4d	3	2	6	Yes by R_1	—	Both polarities

3. Modified TT Circuits with Low-Pass Output Only

In this section, three alternative forms of the circuit shown in Fig. 3(c) and realizing only low-pass response are summarized. The three circuits are shown in Figs. 4(a)–4(c) and they are equivalent to each other.¹⁶ The transfer function of the inverting low-pass is given by

$$\frac{V_{LP}}{V_I} = \frac{\frac{-1}{C_1 C_2 R_2 R_4}}{s^2 + s \left(\frac{1}{C_1 R_1} - \frac{1}{C_2 R_5} \right) + \frac{1}{C_1 C_2} \left(\frac{1}{R_2 R_3} - \frac{1}{R_1 R_5} \right)}. \quad (14)$$

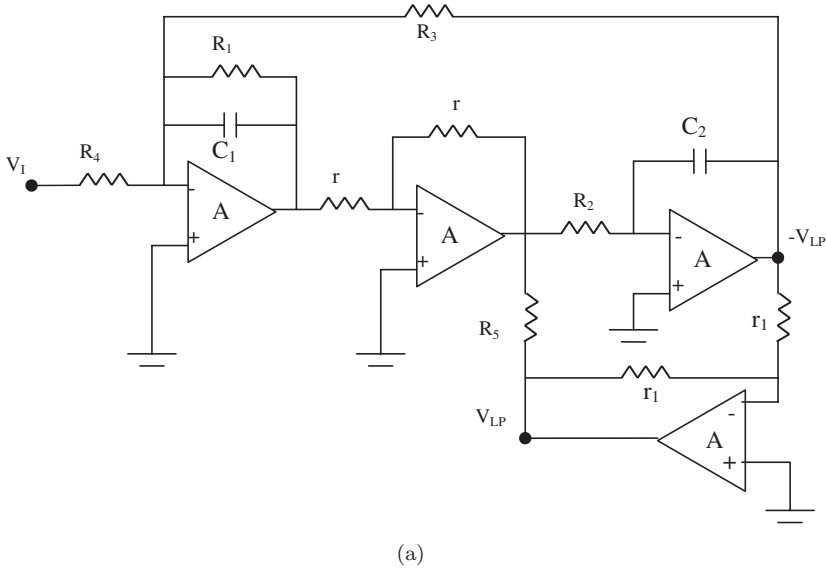
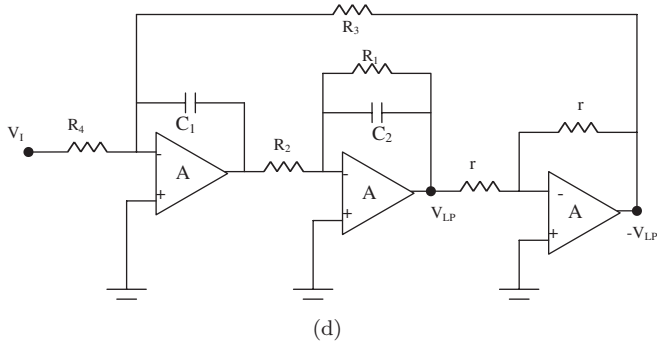
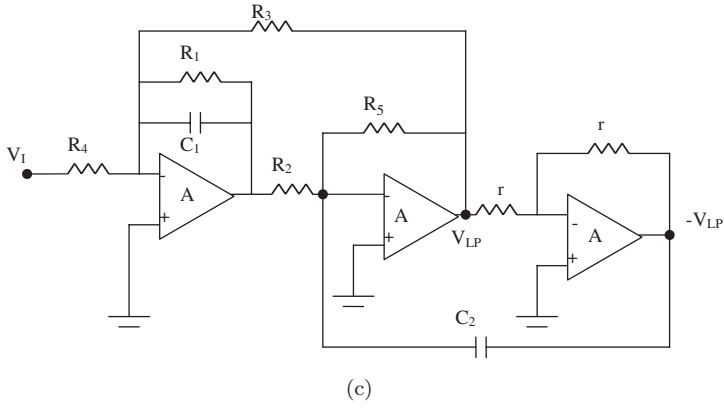
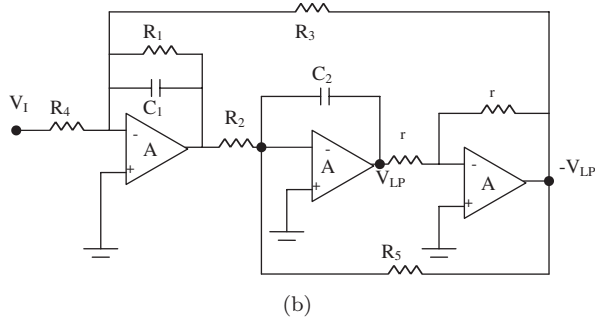


Fig. 4. (a) A modified form of the circuit in Fig. 3(b).¹⁶ (b) A simplified circuit in (a).¹⁶ (c) Alternative equivalent circuit to (a) and (b).¹⁶ (d) Alternative form of Tow–Thomas circuit realizing low-pass only.¹⁷

Fig. 4. (*Continued*)

Another alternative form of TT circuit obtained by interchanging the positions of the lossless and the lossy integrators in the feedback loop of the circuit in Fig. 2(b) is shown in Fig. 4(d).¹⁷ This circuit realizes only low-pass responses with both polarities. Its transfer function is given by

$$\frac{V_{LP}}{V_I} = \frac{\frac{1}{C_1 C_2 R_2 R_4}}{s^2 + \frac{s}{C_2 R_1} + \frac{1}{C_1 C_2 R_2 R_3}}. \quad (15)$$

Compared with the three equivalent low-pass filters described by Eq. (14), it can be seen that this circuit has independent control on Q by varying R_1 which cannot be achieved with any of the three equivalent circuits in Figs. 4(a)–4(c).

4. Frequency Limitation Equations

In Refs. 6 and 17 the single-pole model of the op amp is taken into consideration and the op amp gain is represented by

$$A(s) = \frac{\omega_t}{s}, \quad (16)$$

ω_t is the gain bandwidth product of the op amp.

It was proved in Ref. 6 that the actual ω_0 and Q for the circuit shown in Fig. 4(d) are given as

$$\frac{\Delta\omega_0}{\omega_0} = -\frac{\omega_0}{\omega_t}, \quad (17)$$

$$\frac{\Delta Q}{Q} = \frac{4\omega_0 Q}{\omega_t}. \quad (18)$$

The above equations indicate that the deviation in ω_0 is very limited whereas the major deviation is in Q . Equation (18) can be used to find the maximum frequency of operation of the circuit for a specified op amp, ω_0 and Q and the allowable ΔQ . The above equations apply also to the circuits in Figs. 2(b) and 3(b).

Thus, it is seen that it is desirable to have phase compensation for the Tow–Thomas circuit and its modified versions.

Thomas has shown that² the total phase lag around the loop is related to the Q factor by

$$\phi = -\frac{1}{Q_a} = -\frac{1}{Q} + \frac{4\omega_0}{\omega_t}, \quad (19)$$

Q_a is the actual quality factor and Q is the ideal pole Q . The above result is exactly the same as given by Eq. (18).

5. Compensation of the TT Circuit

There are two types of compensation, passive compensation and active compensation. Before discussing these two types of compensation it is worth to mention the self-compensated TT circuit reported in Ref. 18 which reduces the total phase lag around the loop to $(2\omega_0/\omega_t)$ which is half the value given by Eq. (19) by just changing one circuit connection as shown in Fig. 5(a).¹⁸

5.1. Passive compensation

Thomas² added a compensating capacitor in parallel with one of the loop resistances to produce an amount of phase lead equal to $4\omega_0/\omega_t$ so that phase correction around

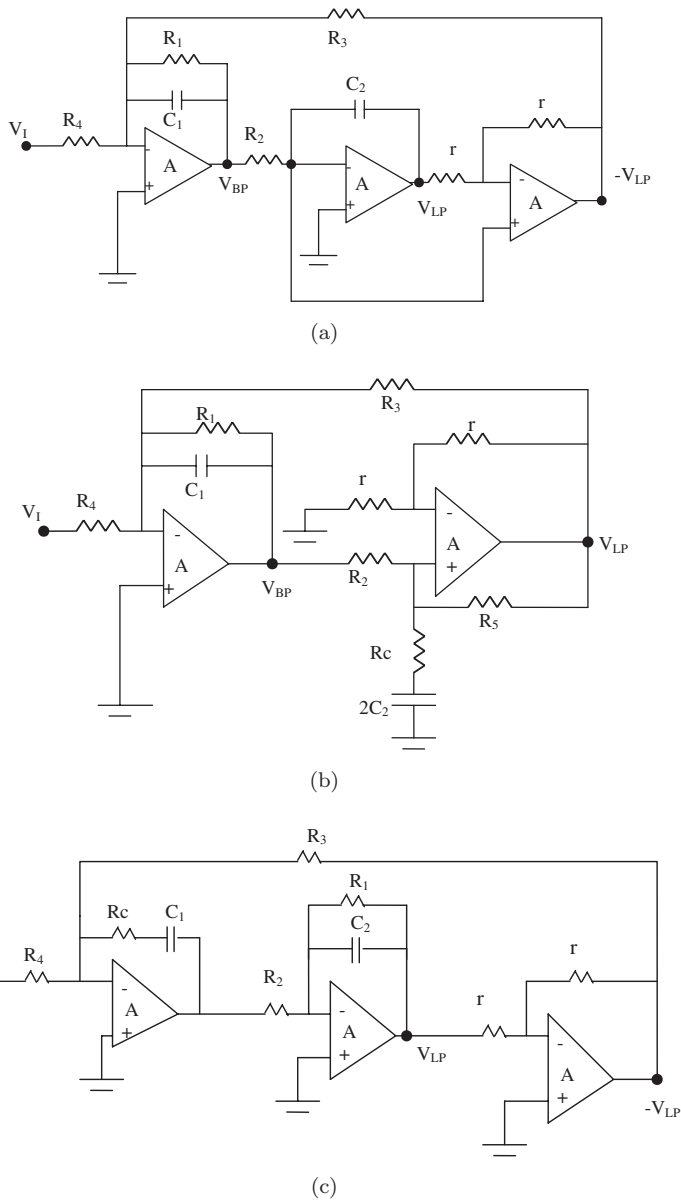


Fig. 5. (a) Partial compensation of the TT circuit using feed-forward technique.¹⁸ (b) Passive compensation applied to the circuit in Fig. 3(d).¹⁹ (c) Passive compensation applied to the circuit in Fig. 4(d).¹⁹

the loop is achieved. Other forms of passive compensation were given in Ref. 19 based on adding a single compensating resistor with one of the two capacitors to realize a phase-lead integrator. Adjusting the phase lead of the integrator will result in a perfect compensation for the unwanted phase shift produced by the op amp

pole. Figure 5(b) represents one of the circuits given in Ref. 19 where R_c represents the compensating resistor added in series with the capacitor $2C_2$ of the Deboo integrator. The design value for R_c is given by $3/(2C\omega_t)$. Figure 5(c) represents another form of passive compensation given in Ref. 19, where R_c represents the compensating resistor added in series with the capacitor C_1 of the inverting integrator. For phase compensation the design value for R_c is given by $4/(C\omega_t)$.

5.2. Active compensation

Several methods of active compensation of the two integrator loop filters will be summarized in this section. The first method is based on replacing the lossless integrator in the circuit in Fig. 2(b) by a phase-lead inverting integrator as shown in Fig. 6(a).²⁰ The excess phase of this integrator is given by

$$\phi \approx \frac{K\omega_0}{\omega_t} \left(\frac{a}{K+1} - 1 \right). \quad (20)$$

Thus, it is seen that the resistor R/a controls the phase of the integrator which can be made leading. The resistor KR controls the integrator stability. Taking the second op amp pole into consideration it is seen that taking $K = 1$ will ensure the integrator stability.²⁰ In this case a is taken equal to 8 to provide a phase lead of $3\omega_0/\omega_t$ which is the amount necessary for phase correction at ω_0 .

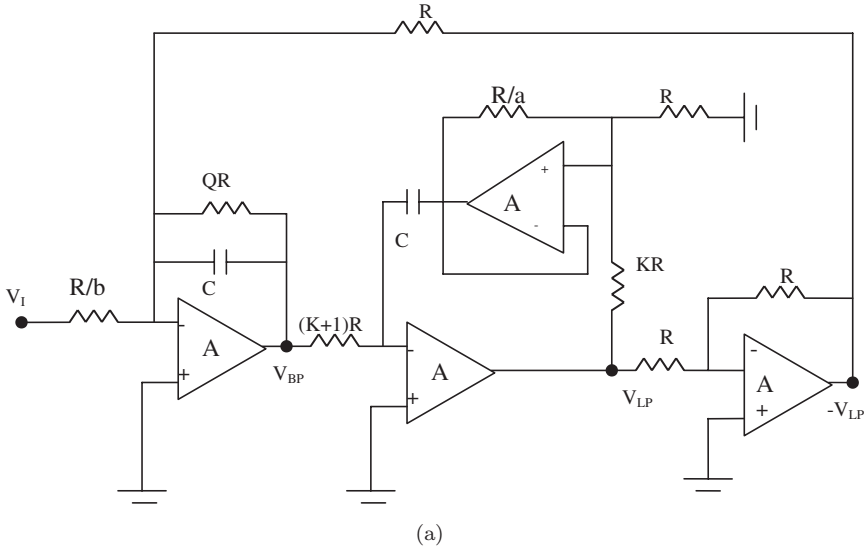
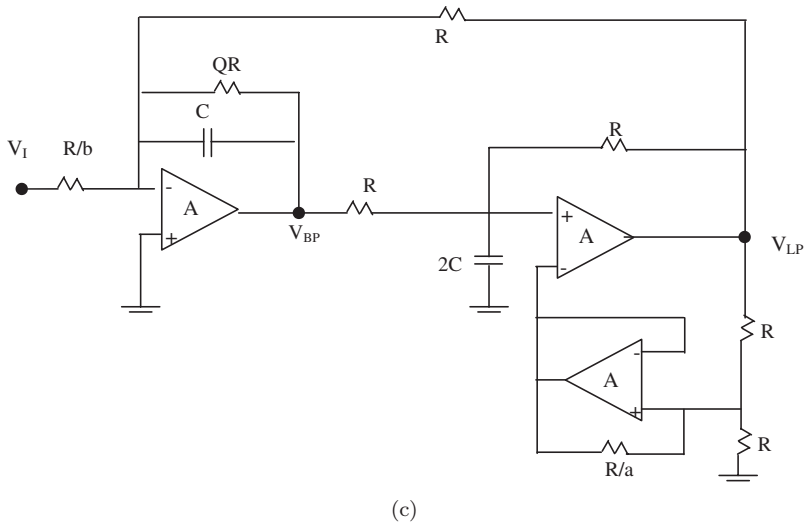
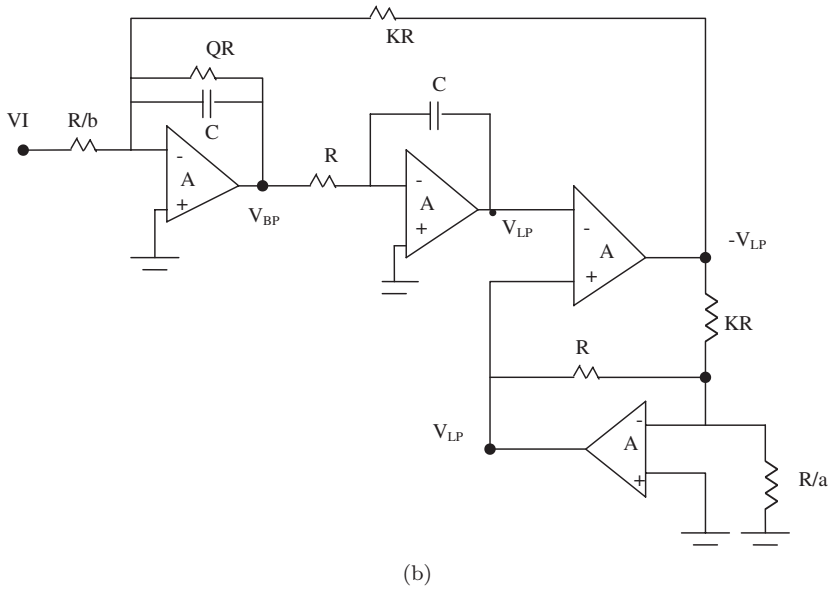


Fig. 6. Active compensated Tow–Thomas circuit using phase-lead (a) inverting integrator,²⁰ (b) inverting amplifier,²¹ and (c) Deboo integrator.²² (d) The Akerberg–Mossberg active compensated TT circuit.^{23–25} The active compensated TT circuit using phase-lead (e) inverting amplifier²⁶ and (f) inverting amplifier.²⁷

Fig. 6. (*Continued*)

An alternative active compensated circuit is given in Fig. 6(b) which represents another active compensated version of Tow-Thomas circuit suitable for high Q and high frequencies and using a phase-lead inverting amplifier to replace the unity gain inverter stage.²¹ To provide the amount of phase lead necessary for phase correction around the loop, a is taken as

$$a = K + 1 - \frac{1}{K}. \quad (21)$$

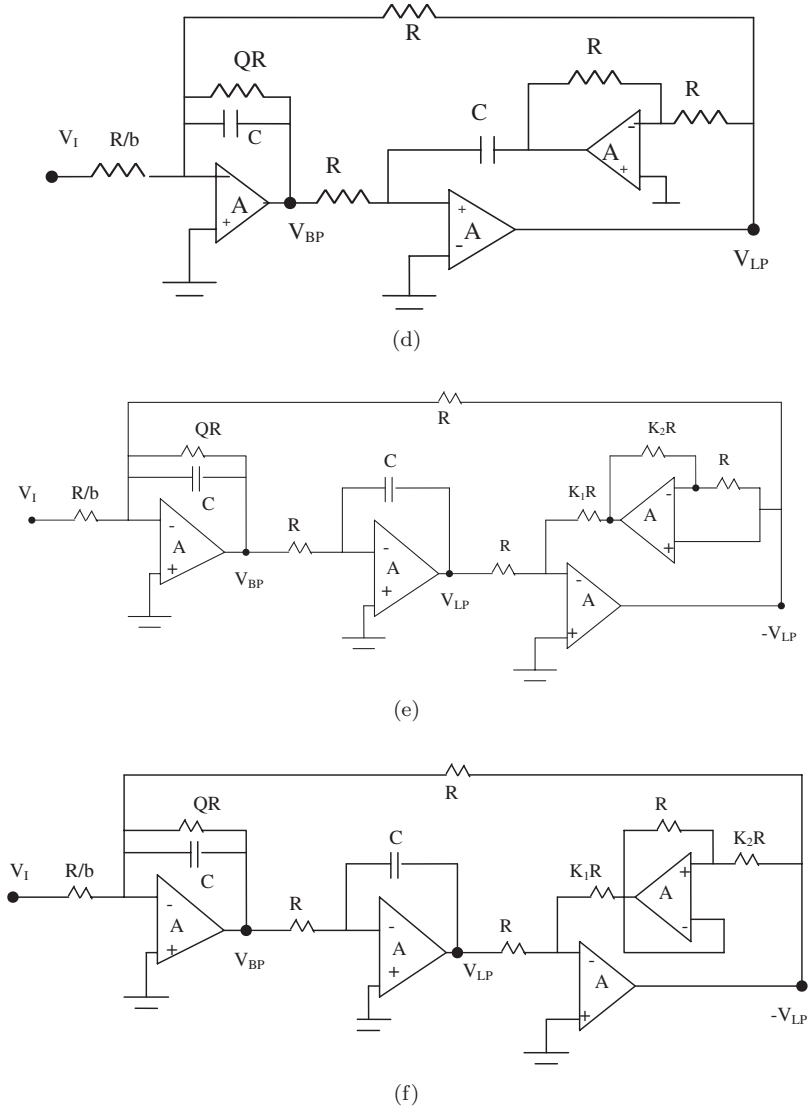


Fig. 6. (Continued)

Taking $K = 2$, results in an unconditionally stable inverting amplifier,²¹ in this case $a = 2.5$.

The active compensated circuit in Fig. 6(c) is based on using a phase-lead Deboo integrator²² adjusted to have a phase lead equal to (ω_0/ω_t) , in this case the parameter a in the circuit in Fig. 6(c) is taken equal to 4. A well-known active compensated TT circuit is shown in Fig. 6(d) which was introduced in Ref. 23 and known by the Akerberg–Mossberg circuit and it is included in some textbooks also.^{23–25} In Ref. 25, however, the second op amp polarity should be reversed. Two

equivalent active compensated TT circuits using phase-lead inverting amplifiers are given in Figs. 6(e) and 6(f).^{26,27} The phase of the inverting amplifier at ω_0 is given $(K_2 - K_1)\omega_0/\omega_t$, thus for $K_1 = 1$, K_2 is taken equal to 3 to provide the necessary phase lead of $2\omega_0/\omega_t$. Another circuit based on applying active phase compensation separately to the Miller integrator and to the Deboo integrator given in Ref. 22 which uses an additional op amp in the feedback loop of the Miller integrator.²⁸ Another variable-phase inverting amplifier that has been used for phase correction in the Tow–Thomas circuit is given in Ref. 29.

6. Spice Simulations

In this section, Spice simulations are carried out using the op amp $\mu\text{A } 741$ from Analog Devices with $f_t = 1 \text{ MHz}$ and biased with supply voltages of $\pm 15 \text{ V}$.

The TT circuit in Fig. 2(b) is designed for $Q = 10$ and $f_0 = 15.92 \text{ kHz}$ taking $C_1 = C_2 = 500 \text{ pF}$, $R_2 = R_3 = R_4 = r = 20 \text{ k}\Omega$ and $R_1 = 200 \text{ k}\Omega$. Figure 7(a) represents the Spice simulation results of the magnitude and phase of the TT circuit in Fig. 2(b) together with the ideal response. It is seen that the Q has increased drastically from its theoretical value of 10. From Fig. 7(a) Spice simulation results of the Tow–Thomas circuit in Fig. 2(b) simulation results $\Delta Q/Q = 0.73$ which is slightly higher than the theoretical expected value obtained from Eq. (18) as

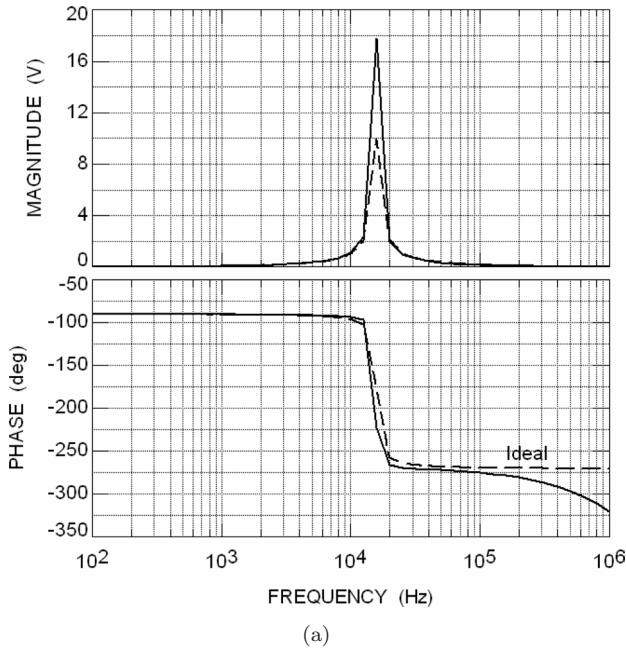


Fig. 7. Spice simulation results of (a) the Tow–Thomas circuit in Fig. 2(b), (b) the circuit in Fig. 3(b), (c) the circuit in Fig. 3(d), and (d) the circuit in Fig. 4(d).

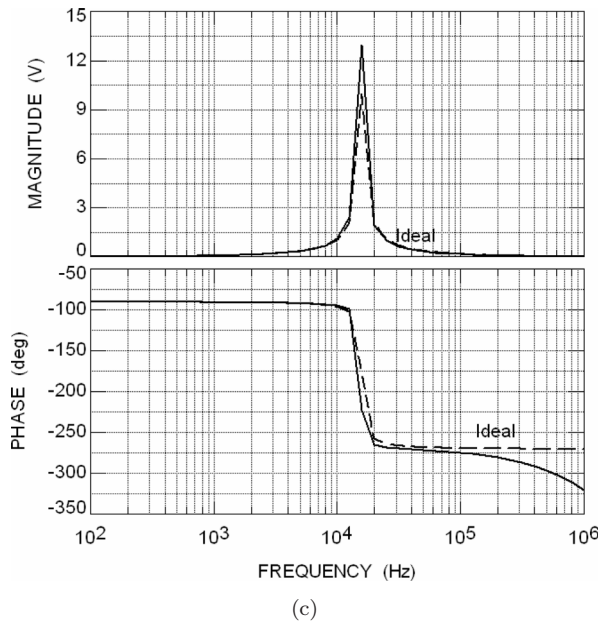
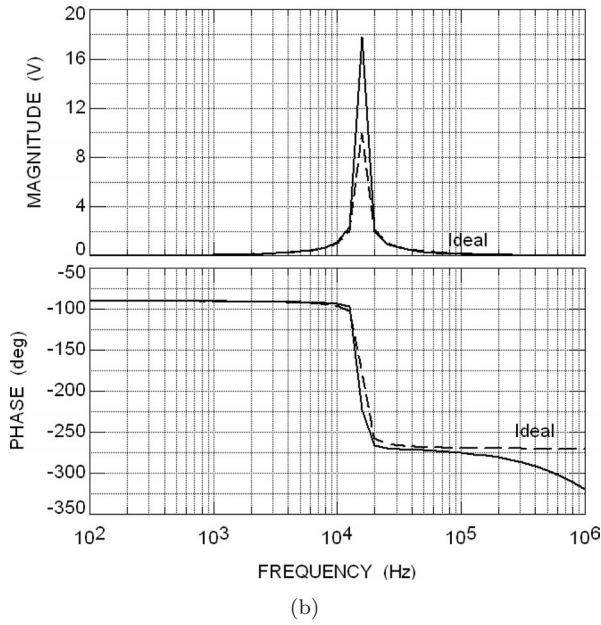


Fig. 7. (Continued)

0.64. Figure 7(b) represents the Spice simulation results of the magnitude and phase of the TT circuit in Fig. 3(b) designed with the same values as the previous circuit together with the ideal response. It is seen that the $\Delta Q/Q$ is the same as in the circuit in Fig. 2(b). Figure 7(c) represents the Spice simulation results of the

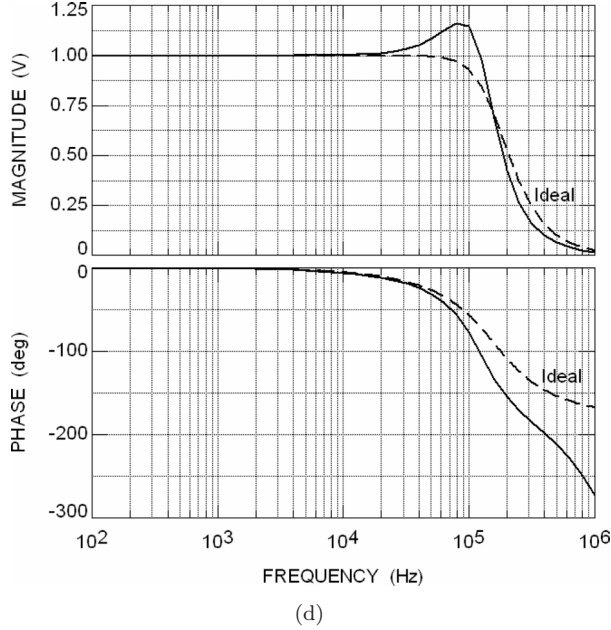


Fig. 7. (Continued)

magnitude and phase of the TT circuit in Fig. 3(d) designed with $C_1 = C_2 = 500$ pF, $R_2 = R_3 = R_4 = R_5 = r = 20$ k Ω and $R_1 = 200$ k Ω . It is seen that the $\Delta Q/Q = 0.3$ which is lower than the error in the previous two cases and is very close to the theoretical expected value given by $3\omega_0 Q/\omega_t = 0.48$. The TT circuit in Fig. 4(d) is designed to realize a maximally flat magnitude low-pass response having $Q = 0.707$ and $f_0 = 159.2$ kHz taking $C_1 = C_2 = 50$ pF, $R_2 = R_3 = R_4 = r = 20$ k Ω and $R_1 = 14.14$ k Ω . Figure 7(d) represents the Spice simulated magnitude and phase responses together with the ideal responses. It is seen that there is a peak in the magnitude response due to the Q enhancement effect.

Figure 8(a) represents the Spice simulated magnitude and phase responses together with the ideal responses of the partial compensated circuit in Fig. 5(a). From the simulation results $\Delta Q/Q = 0.25$ which is very close to the theoretical value given by $2\omega_0 Q/\omega_t = 0.32$. Figure 8(b) represents the Spice simulated magnitude and phase responses together with the ideal responses of the passive compensated circuit in Fig. 5(b) based on the addition of the compensating resistor R_c which is taken as 350 Ω to provide perfect compensation. It should be noted that the value taken by R_c is slightly lower than the theoretically calculated value of $3/(2C\omega_t) = 477$ Ω .

The passive compensated TT low-pass filter in Fig. 5(c) is designed to realize a maximally flat magnitude low-pass response taking $Q = 0.707$ and $f_0 = 159.2$ kHz taking all circuit components as before with R_c added and taken as $4/(C\omega_t) = 12.74$ k Ω . Figure 8(c) represents the magnitude and phase simulation

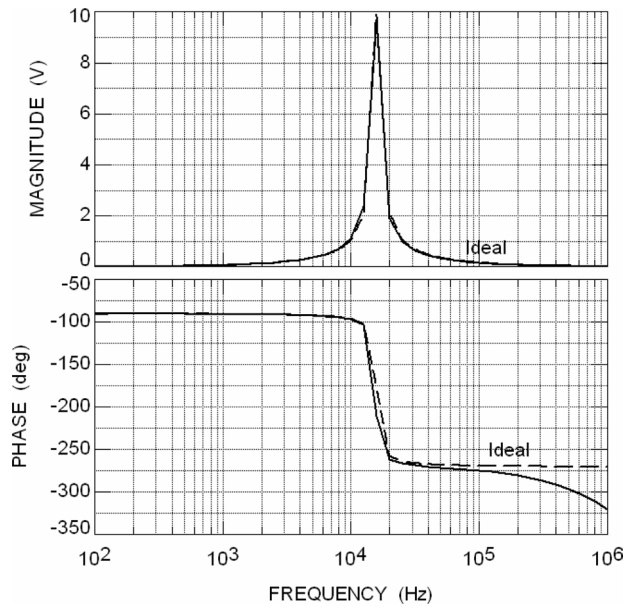
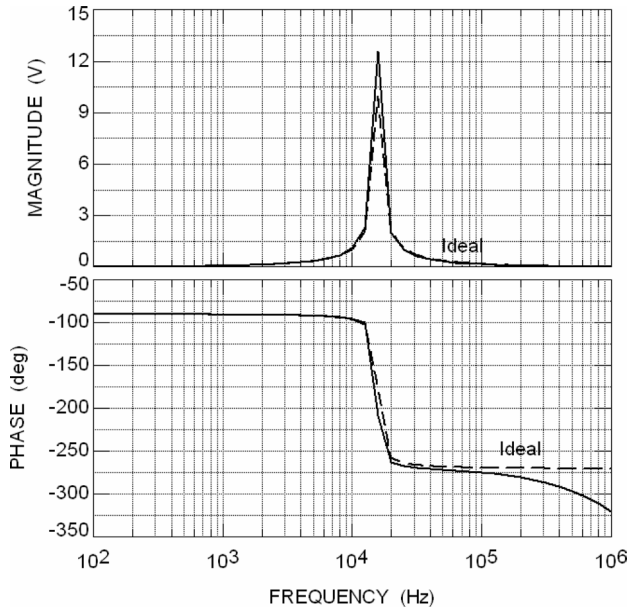
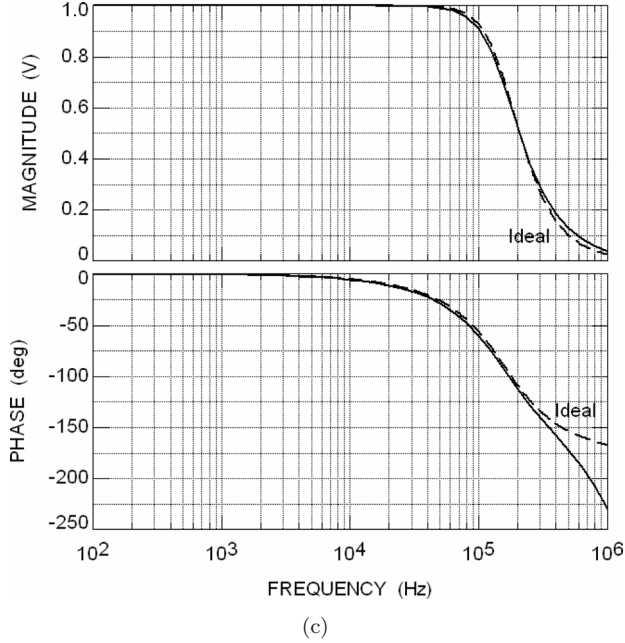


Fig. 8. Spice simulation results of (a) the partial-compensated TT circuit in Fig. 5(a), (b) the passive-compensated TT circuit in Fig. 5(b), and (c) the passive-compensated TT circuit in Fig. 5(c).

Fig. 8. (*Continued*)

results together with the ideal responses. It is seen that the response is very close to the ideal one indicating a perfect passive compensation.

Next, the simulation results for three of the active-compensated circuits designed for $Q = 10$ and $f_0 = 15.92$ kHz and taking $b = 1$, $C = 500$ pF, $R = 20$ k Ω are given.

Figure 9(a) represents the Spice simulated magnitude and phase responses together with the ideal responses of the active-compensated circuit in Fig. 6(a), the resistor $(K + 1)R$ is taken as 40 k Ω and the resistor (R/a) is taken as 2.5 k Ω .

Figure 9(b) represents the Spice simulated magnitude and phase responses together with the ideal responses of the active-compensated circuit in Fig. 6(b), taking $K = 2$, in this case and for phase compensation $a = 2.5$. The resistor R/a is taken as 8.5 k Ω which is slightly higher than its calculated value of 8 k Ω for perfect compensation.

Figure 9(c) represents the Spice simulated magnitude and phase responses together with the ideal responses of the circuit in Fig. 6(d).

The active-compensation simulation results in all of the provided three simulations agree well with the ideal responses as seen from Figs. 9(a)–9(c).

7. Conclusions

The history of Tow–Thomas second-order filter is reviewed. Two alternative generation methods of the Tow–Thomas filter are discussed. The first is a generation method from the second-order passive RLC filter and the second is from the multiple

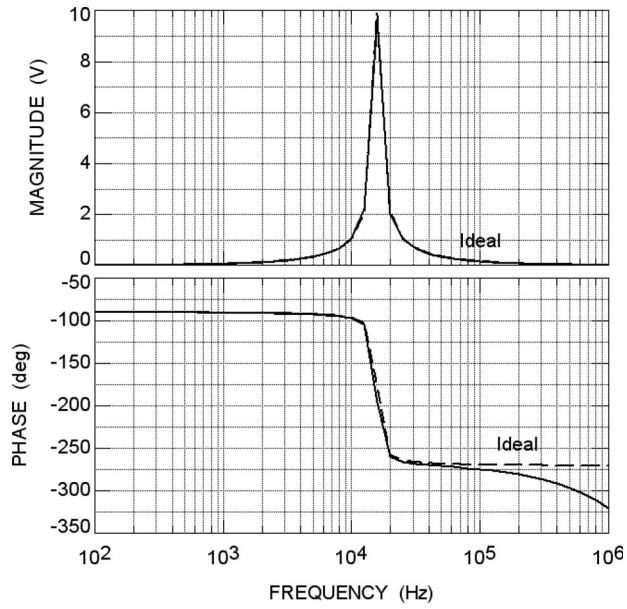
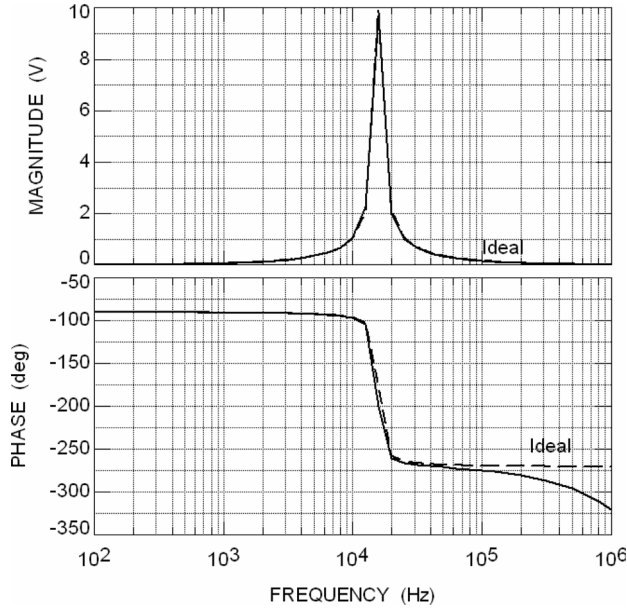


Fig. 9. Spice simulation results of (a) the active-compensated Tow–Thomas circuit in Fig. 6(a), (b) the active-compensated Tow–Thomas circuit in Fig. 6(b), and (c) the Akkerberg–Mossberg circuit in Fig. 6(d).

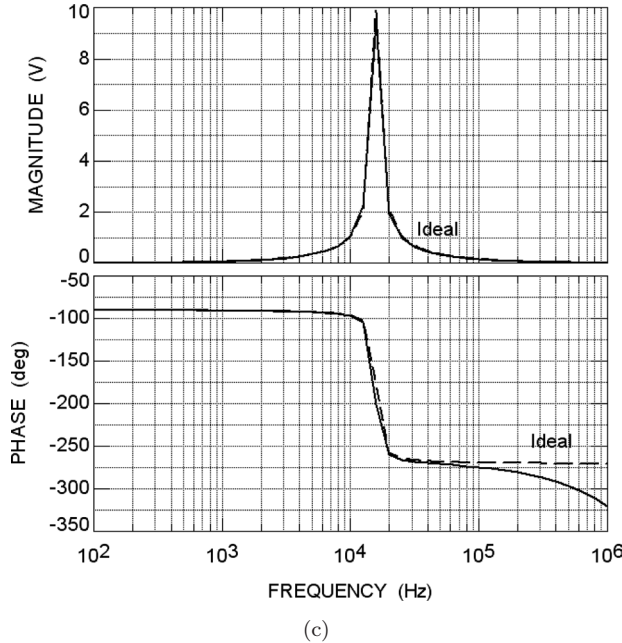


Fig. 9. (Continued)

feedbacks inverting low-pass filter using a single op amp. Several forms of the circuit are briefly reviewed.

Table 1 summarizes the polarities of the realizable outputs and the number of circuit components in each of the circuits. The original Tow–Thomas circuit has independent control on Q , some of the modified circuits lose this very important feature as summarized in Table 1.

Although the Tow–Thomas circuit has very low passive sensitivities to all passive circuit components, it suffers from a rather drastic Q -factor enhancement effect due to the op amp finite gain bandwidth. Partial-phase compensation which reduces the phase lag around the loop to half its value by just changing one connection has been discussed with simulation results. Passive and active compensation methods to improve the circuit performance for high- Q designs are summarized. Spice simulation results are included. The passive and active compensation simulation results agree well with the ideal responses as seen from the simulation results.

Acknowledgment

The author thanks the reviewers for their useful comments.

References

1. J. Tow, A step by step active filter design, *IEEE Spectrum* **6** (1969) 64–68.
2. L. Thomas, The biquad: Part I — Some practical design considerations, *IEEE Trans. Circuit Theor.* **CT-18** (1971) 350–357.

3. G. Daryanani, *Principles of Active Network Synthesis and Design* (Wiley, 1976), pp. 339–358.
4. M. S. Ghausi and K. R. Laker, *Modern Filter Design, Active RC and Switched Capacitor* (Prentice Hall, Engelwood Cliffs, NJ, 1981), pp. 226–227.
5. M. E. Van Valkenburg, *Analog Filter Design* (Holt Rinehart and Winston, 1982), pp. 136–137.
6. A. Budak, *Passive and Active Network Analysis and Synthesis* (Houghton Mifflin, 1974), pp. 356–365.
7. A. S. Sedra and K. C. Smith, *Microelectronic Circuits* (Oxford University Press, 1998), pp. 927–929.
8. H. Y.-F. Lam, *Analog and Digital Filters* (Prentice Hall, 1979), pp. 401–417.
9. L. P. Huelsman and P. E. Allen, *Introduction to Theory and Design of Active Filters* (McGraw Hill, 1980), pp. 258–269.
10. S. K. Mitra, *Active Inductorless Filters* (IEEE Press, 1971).
11. A. M. Soliman, New inverting–non-inverting band-pass and low-pass biquad circuit using current conveyors, *Int. J. Electron.* **81** (1996) 577–583.
12. H. O. Elwan and A. M. Soliman, A novel CMOS differential voltage current conveyor and its applications, *IEE Proc. Circuits Dev. Syst.* **144** (1997) 195–200.
13. W. Chiu, S. I. Liu, H. W. Tsao and J. J. Chen, CMOS differential difference current conveyors and their applications, *IEE Proc. Circuits Dev. Syst.* **143** (1996) 91–96.
14. P. R. Geffe, RC amplifier resonators for active filters, *IEEE Trans. Circuit Theor.* **CT-15** (1968) 415–419.
15. A. M. Soliman, Generation of CCH and CFOA filters from passive RLC filters, *Int. J. Electron.* **85** (1998) 293–312.
16. P. V. A. Mohan, V. Ramachandran and M. N. Swamy, Nodal voltage simulation of active RC networks, *IEEE Trans. Circuits Syst.* **32** (1985) 1085–1088.
17. A. Budak and D. Petrala, Frequency limitations of active filters using operational amplifiers, *IEEE Trans. Circuit Theor.* **CT-19** (1972) 322–328.
18. P. O. Brackett and A. S. Sedra, Active compensation for high frequency effects in op amp circuits with applications to active filters, *IEEE Trans. Circuits Syst.* **CAS-23** (1976) 68–72.
19. A. M. Soliman and M. Ismail, Phase correction in two integrator loop filters using a single compensating resistor, *Electron. Lett.* **14** (1978) 375–376.
20. A. M. Soliman, Novel phase lead inverting integrator and its application in two integrator loop filters, *Electron. Lett.* **16** (1980) 475–476.
21. A. M. Soliman, Novel two op amps three resistor variable phase inverting amplifier, *Electron. Lett.* **16** (1980) 294–295.
22. A. M. Soliman, Two integrator loop filters with stable Q factor, *Frequenz* **35** (1981) 19–22.
23. D. Akerberg and K. Mossberg, A versatile active RC building block with inherent compensation for the finite bandwidth of the amplifier, *IEEE Trans. Circuits Syst.* **CAS-21** (1974) 75–78.
24. A. S. Sedra and P. O. Brackett, *Filter Theory and Design: Passive and Active* (Matrix Publishers, Illinois, 1978), pp. 568–571.
25. T. Deliyannis, Y. Sun and J. K. Fidler, *Continuous Time Active Filter Design* (CRC Press, 1999), pp. 146–147.
26. A. M. Soliman and M. Ismail, A universal variable phase 3-port VCVS and its applications in two integrator loop filters, *Proc. IEEE Int. Symp. Circuits and Systems*, Houston, Texas (1980), pp. 83–86.

27. M. Ismail and A. M. Soliman, A novel active compensation method of op amp VCVS and weighted summer building blocks, *Proc. IEEE Int. Symp. Circuits and Systems*, Tokyo, Japan (1979), pp. 922–925.
28. P. W. Vogel, Method for phase correction in active RC circuits using two integrators, *Electron. Lett.* **7** (1971) 273–275.
29. A. M. Soliman, Phase correction in two integrator loop filters using new variable phase inverting amplifier, *Electron. Lett.* **16** (1980) 186–188.